

# Convection in binary fluid mixtures: A model of four coupled amplitudes

B. Huke and M. Lücke

*Institute of Theoretical Physics, Saarland University, Postfach 15 11 50, 66041 Saarbrücken, Germany*

E-mail: huke@lusi.uni-sb.de

We consider the bifurcation scenario that is found in Rayleigh–Bénard convection of binary fluid mixtures like ethanol–water at positive separation ratios and small Lewis numbers leading to a bifurcation sequence of square, oscillatory crossroll, stationary crossroll, and roll patterns. We propose a system of four coupled amplitudes that is capable to model all important properties.

**Key words:** Rayleigh–Bénard convection, Soret effect, pattern selection, amplitude equations

**PACS numbers:** 47.20.Bp; 47.20.Ky; 47.54.-r

## 1 Introduction

The Rayleigh–Bénard system [1, 2] is one of the most popular model systems to study spontaneous structure formation emerging via instabilities. The system consists of a fluid layer confined between two parallel plates perpendicular to the direction of gravity, and exposed to a vertical temperature gradient that is established by keeping the upper and lower plate at two different temperatures  $T_0 - \Delta T/2$  and  $T_0 + \Delta T/2$  respectively.

Rayleigh–Bénard convection in one-component fluids at small and moderate temperature differences is well understood, mainly thanks to the work of Busse and co-workers in the 70s and 80s [3, 4, 5, 6]. The bifurcation behavior becomes more complex in binary mixtures. Here, the concentration enters as an additional relevant dynamic field. Concentration differences are created in the presence of a non-vanishing Soret effect, a nonequilibrium effect that describes the driving of concentration currents by temperature differences.

The concentration couples back into the system's dynamics via variations that determine the buoyancy force density. When the lighter component of the mixture is driven into the direction of higher temperature, thereby enhancing the density gradient and further destabilizing the layer one speaks of

a positive Soret effect, and of a negative Soret effect in the opposite case.

Convection in binary mixtures shows a very rich bifurcation behavior. For negative separation ratios convection rolls bifurcate backwards and time-dependent patterns, namely traveling waves and standing waves appear. The bistability of convective patterns and the ground state leads to the existence of localized structures and fronts.

In the case of positive separation ratios on which we will focus in this paper the two-dimensional roll structures are often replaced by squares at onset, but become the preferred pattern at higher temperature differences. For intermediate  $\Delta T$  two types of crossroll structures can exist, a stationary and an oscillatory type that transfer stability from squares to rolls.

There are few-mode models that satisfactorily explain the bifurcation properties for negative Soret effects [7]. However, for positive Soret effects a model with only a few degrees of freedom, that is able to properly describe rolls, squares and crossrolls seems to be lacking.

In this paper we will present a system of four equations that describe all important properties of the square – crossroll – roll transition for the case of a positive Soret effect.

The paper is organized as follows: after this in-

introduction we discuss in Sec. 2 the Rayleigh–Bénard system and the bifurcation scenario for positive Soret effects in more detail. In Sec. 3, the main part, we present and discuss a model system that shows a similar behavior but incorporates an additional, artificial symmetry that makes it easier to identify the stationary solutions but leads to some qualitative disagreements with the full system. In Sec. 4 we add some terms that break this symmetry and demonstrate that then these differences disappear. We summarize our findings in Sec. 5 and provide an outlook.

## 2 Bifurcation scenario

The basic equations that couple convection velocity  $\mathbf{u}$ , temperature  $\theta$ , concentration  $c$  and pressure  $P$  read in a dimensionless form [8]

$$\begin{aligned}(\partial_t + \mathbf{u} \cdot \nabla) \mathbf{u} &= -\nabla P + \sigma \left[ (\theta + c) \mathbf{e}_z + \nabla^2 \mathbf{u} \right] \\(\partial_t + \mathbf{u} \cdot \nabla) \theta &= Ru_z + \nabla^2 \theta \\(\partial_t + \mathbf{u} \cdot \nabla) c &= R\psi u_z + L \left( \nabla^2 c - \psi \nabla^2 \theta \right) \\ \nabla \cdot \mathbf{u} &= 0 .\end{aligned}\tag{1}$$

The fields are given as deviations from the quiescent conductive ground state. The direction of gravity is the negative  $z$  direction. See ref. [8] for details. There appear four different parameters in these equations: the Rayleigh number  $R$  is the control parameter, the dimensionless temperature difference between upper and lower plate. In pure fluids, the critical Rayleigh number of the onset of convection is  $R_c(\psi = 0) = 1707.76$ . One defines a reduced Rayleigh number  $r = R/R_c(\psi = 0)$ . The Prandtl number  $\sigma$  is the ratio of the timescales of heat and momentum diffusion. The Lewis number  $L$  on the other hand is the ratio of the heat and concentration timescales. The separation ratio  $\psi$  finally measures the strength of the Soret effect. In the conductive ground state it determines the ratio of the density gradients due to concentration and temperature.

In typical liquids it is  $\sigma \approx 10$ . Concentration diffusion is slow in ordinary liquid mixtures; a typical value for  $L$ , say, for ethanol–water is 0.01.  $\psi$

varies with the mean concentration and mean temperature and can be both positive and negative in ethanol–water.

For positive  $\psi$  three different bifurcation scenarios exist at small and moderate  $r$ . (i) For very small  $\psi$  and relatively large  $L$  the Soret generated concentration variations are small and easily diffused away. The mixture then still behaves qualitatively like a pure fluid. The first convection structure to be observed above onset takes the form of parallel, stationary rolls with alternating direction of rotation. Near onset,  $u_z$ ,  $\theta$ , and  $c$  can be described by a function  $A \cos(kx) f(z)$  with  $k$  being the wavenumber of the rolls and  $f(z)$  being different for the three fields and defining the critical vertical profile.

(ii) When  $\psi$  is larger and/or  $L$  is smaller the mixture begins to behave qualitatively different. The rolls are replaced by a square pattern near onset that can be written as a linear combination of equally strong rolls in  $x$ - and  $y$ -direction, i. e.,  $[A \cos(kx) + B \cos(ky)] f(z)$  with  $A = B$ . At higher  $r$  however the advective mixing is strong enough to equilibrate the concentration field outside of some small boundary layers at the plates and between the rolls. The mixture again behaves like a pure fluid and squares lose their stability to rolls. The stability is transferred via a crossroll branch, a structure that, like squares, can be understood as a superposition of two perpendicular sets of convection rolls. In the case of crossrolls, however, the two amplitudes  $A$  and  $B$  are not equal and the crossroll structure therefore lacks the square  $x \leftrightarrow y$  symmetry. Like squares and rolls, these structures are stationary.

(iii) At even smaller  $L$ , but easily realizable with liquid mixtures the scenario is again different as shown in Fig. 1. There the squared amplitude of the leading velocity mode of the  $x$ -roll set is plotted versus the reduced Rayleigh number  $r$ . Solid (open) symbols denote stable (unstable) structures. Squares (square symbols) are again stable at small  $r$  but lose their stability against another type of crossrolls, an oscillatory one (lines without symbols). The bifurcation point where the stationary crossrolls (triangles) emerge still exists but at higher  $r$ , where the oscillatory instability has already taken place. In the oscillatory crossroll branch the ampli-

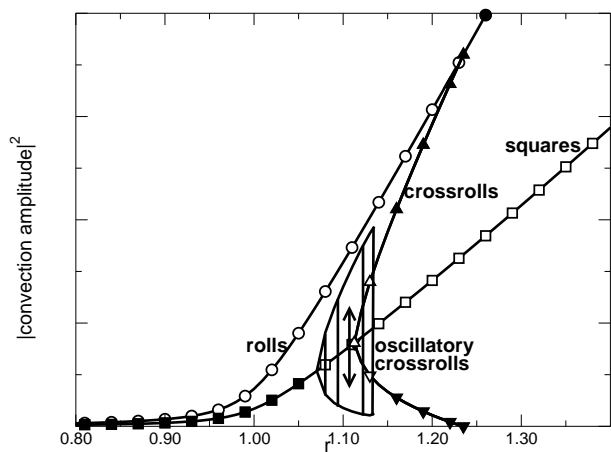


FIG. 1. Bifurcation scenario of the full hydrodynamic field equations for  $\sigma = 27$ ,  $L = 0.0045$ ,  $\psi = 0.23$ . The wave number of the structures is  $k = \pi$ .

tude of the  $x$ - and  $y$ -roll set varies periodically in counterphase to each other such that when at one time the  $x$ -rolls are stronger, half a period later the  $y$ -rolls will be the stronger set. The two branches in Fig. 1 show the maximal and minimal amplitudes of these time dependent structures. The two stationary crossroll branches represent the two different types: In the upper branch the  $x$ -roll component is the dominant one and their amplitude grows whereas the amplitude of the  $y$ -roll component gets smaller. When the latter component vanishes the crossroll ends at a bifurcation point on the  $x$ -roll branch (circles). The lower branch belongs to the type of crossrolls where the  $y$ -roll component is the dominant one. Now the plotted  $x$ -roll component gets smaller until the structure ends on the  $y$ -roll branch, i. e., on the axis in Fig. 1 since there only the strength of the  $x$ -rolls is plotted. The stationary crossrolls gain stability when the oscillatory crossrolls vanish and transfer the stability to the rolls. The existence of all these structures have been demonstrated in experiments [9, 10, 11].

The time-dependence of  $A$  and  $B$  is plotted for two oscillatory crossrolls in Fig. 2. It shows the main characteristics of these structures near the beginning and the end of their  $r$ -range of existence. While the oscillation is very harmonic at smaller  $r$  it becomes very anharmonic at higher  $r$ . The frequency decreases. Finally, the oscillatory crossrolls

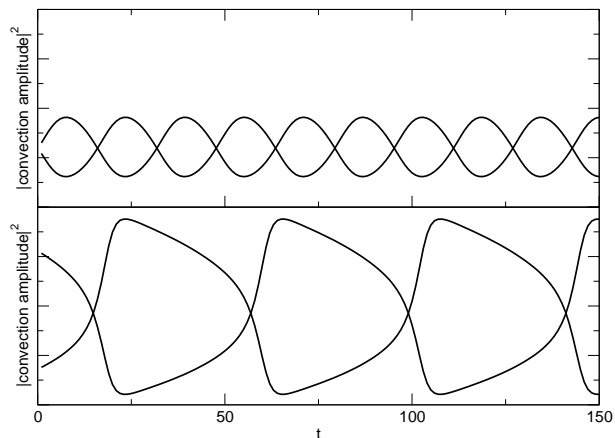


FIG. 2. Oscillatory crossrolls, squared amplitude of the  $x$ - and  $y$ -roll component for the parameters of Fig. 1 and  $r = 1.08$  (top),  $r = 1.13$  (bottom).

end in an entrainment process in a very narrow  $r$ -interval [12].

The crossroll structures exist around  $r = 1$ , i. e. the critical Rayleigh number of the pure fluid. In the same region the branches of rolls and squares bend upwards. Before and after this transition interval the curves are almost linear but with very different slopes. These two regimes at small and large  $r$  are called the Soret and the Rayleigh regime respectively. In the Soret region the convection can be well explained by an amplitude equation model including only cubic terms. In the Rayleigh region on the other hand the concentration field has been equilibrated and the convection amplitudes agree well with those of the pure fluid. In the Rayleigh region slightly above  $r = 1$  the pure fluid still obeys its own amplitude equation and so does therefore indirectly also the mixture [13]. We will make use of the fact that the bifurcation behavior of the mixture can in fact be described by two different amplitude equations in two different  $r$ -intervals in the next section.

### 3 The simplified model

In this section we want to present a first attempt to explain the bifurcation scenario as described above by means of a simple model. The full picture cannot

be captured by simple amplitude equations derived in an expansion around the onset in combination with a multi-scale analysis from the basic equations. Although a sequence of stable squares, forward bifurcating stable (stationary) crossrolls, and finally stable rolls may be described with a system of two coupled quintic amplitude equations [14], the oscillatory crossrolls are not contained in such a model. When  $A$  is the real amplitude of  $x$ -rolls, referring to a critical mode  $A \cos(kx)f(z)$ , and  $B$  is the corresponding mode in  $y$ -direction then a system of two coupled amplitude equations must read for reasons of symmetry

$$\begin{aligned} d_t A &= \mu A - F(A^2, B^2) A, \\ d_t B &= \mu B - F(B^2, A^2) B, \end{aligned} \quad (2)$$

with some arbitrary function  $F$ .  $F$  is real since the critical perturbations lead to stationary patterns. For squares, it is  $A = B$  and the Jacobian of the right hand sides of the above equations will be symmetric. Therefore, complex eigenvalues that would mark the appearance of oscillatory crossrolls are not possible along this branch.

In order to reflect the existence of the Soret and Rayleigh regime we construct a model of two coupled sets of amplitude equations. We define two different amplitudes  $A_1$  and  $A_2$ , both describing rolls in  $x$ -direction of different nature: solutal rolls that exist in the Soret region due to the destabilizing effect of the initial concentration gradient and which are described by a mode  $A_1 \cos(kx)f(z)$  and the thermal rolls  $A_2 \cos(kx)g(z)$  that exist in the Rayleigh regime environment of almost homogeneous concentration and which are driven by the thermal stress alone.  $B_1$  and  $B_2$  are the corresponding amplitudes for the rolls in  $y$ -direction.

The most simple model would consist of two sets of equations as in (2), including only cubic terms to couple the  $A$ - and  $B$ -rolls and additional cubic terms to couple the index 1 and index 2 structures:

$$\begin{aligned} d_t A_1 &= \mu_1 A_1 \\ &\quad - A_1(b_1 A_1^2 + c_1 B_1^2 + d_1 A_2^2 + e_1 B_2^2), \\ d_t A_2 &= \mu_2 A_2 \end{aligned}$$

$$\begin{aligned} &\quad - A_2(b_2 A_2^2 + c_2 B_2^2 + d_2 A_1^2 + e_2 B_1^2), \quad (3) \\ d_t B_1 &= \mu_1 B_1 \\ &\quad - B_1(b_1 B_1^2 + c_1 A_1^2 + d_1 B_2^2 + e_1 A_2^2), \\ d_t B_2 &= \mu_2 B_2 \\ &\quad - B_2(b_2 B_2^2 + c_2 A_2^2 + d_2 B_1^2 + e_2 A_1^2). \end{aligned}$$

These equations do not define an amplitude equation model in a strict sense since they are not meant to result from a controlled expansion of the dynamics near the bifurcation threshold of the full system. Instead, in order to describe the actual convection behavior we have two bifurcation points here, as it is displayed by the two different control parameters  $\mu_1$  and  $\mu_2$ . These parameters are not independent however. Since the only control parameter in the Rayleigh-Bénard system is  $r$ , the parameters  $\mu_i$  must be functions of each other. We set

$$\mu_1 = \mu, \quad \mu_2 = a\mu - \mu_0. \quad (4)$$

The two bifurcation points are at  $\mu_1 = 0$  and at  $\mu_2 = 0$ . Since for  $L \ll 1$  solutal rolls grow on a much slower timescale than thermal rolls one has to have  $a \gg 1$ . When  $\mu = -1$  refers to  $r = 0$  it has to be  $\mu_2 = 0$  at  $\mu \gg 1$  since the onset of convection in mixtures lies at much smaller  $r$  than the onset  $r = 1$  in a pure fluid. For the plots we set  $a = 10$  and  $\mu_0 = 100$ . That means that the timescale of the solutal rolls is assumed 10 times larger than the one of the thermal rolls. The latter appear only at  $\mu > 10$ , or 11 times the critical Rayleigh number of the solutal rolls. The ratios found in the numerical investigation of the full system are typically even larger for realistic parameter combinations.

We assume all parameters  $b_1, b_2, \dots, e_2$  to be positive. A different sign of any of these would lead to unwanted features in the bifurcation scenario. Since  $a \gg 1$  we can assume that for any two parameters  $p, q \in \{b_1, b_2, \dots, e_2\}$  the inequality  $p < aq$  holds. This assumption will simplify our discussion below. We can set  $b_1 = b_2 = 1$  by normalizing the amplitudes accordingly.

The equations (3) show several symmetry properties. They are invariant under an exchange of  $A$  and  $B$  amplitudes, i.e., under exchange of  $x$  and  $y$ . The absence of quadratic terms guarantees the

preservation of the upflow–downflow symmetry of the convective fields. A change of the sign of only  $B_1$  and  $B_2$  or only  $A_1$  and  $A_2$  corresponds to a shift of the  $x$ - or  $y$ -rolls by half a wavelength.

Furthermore, it is even possible to change the sign of only one amplitude. However, this symmetry is artificial. The real convection patterns must be considered as a nonlinear superposition of the solutal and thermal patterns. Changing, e. g., in  $x$ -rolls the direction of rotation of the solutal contribution while leaving the thermal one unchanged is certainly not a symmetry operation. Nevertheless we will add terms that break this symmetry of eqs. (3) only in the next section.

Although the bifurcation scenario of the simplified model (3) disagrees qualitatively with that of the full hydrodynamic field equations in some points it nevertheless facilitates to understand some other features. Furthermore, the simplified model easily allows to get analytical solutions for the stationary structures: Every single mode can be set independently to zero. The remaining equations can in the stationary case then be rewritten as a linear system with the squares of the nonzero amplitudes as variables. The unique solution is a linear function of  $\mu$ , and physically relevant in a  $\mu$ -interval where all amplitude squares are  $\geq 0$ . We can conclude that there are at maximum 16 different stationary solutions of eqs. (3) because there are  $2^4$  possible ways to set some amplitudes to zero.

### 3.1 Thermal and solutal rolls

The first kind of structures we discuss are  $x$ -rolls with  $B_1 = B_2 = 0$  as solutions of the subsystem

$$\begin{aligned} d_t A_1 &= \mu_1 A_1 - A_1 (b_1 A_1^2 + d_1 A_2^2) , \\ d_t A_2 &= \mu_2 A_2 - A_2 (b_2 A_2^2 + d_2 A_1^2) . \end{aligned} \quad (5)$$

Since  $b_1, b_2 > 0$ , both pure solutal or  $A_1$ -rolls

$$A_1^2 = \frac{\mu_1}{b_1} , \quad A_2 = 0 \quad (\mu_1 = \mu > 0) , \quad (6)$$

and pure thermal or  $A_2$ -rolls

$$A_2^2 = \frac{\mu_2}{b_2} , \quad A_1 = 0 \quad (\mu_2 = a\mu - \mu_0 > 0) , \quad (7)$$

exist as forward bifurcating solutions. They are plotted in Fig. 3 for  $b_1 = b_2 = 1$  and  $a, \mu_0$  as above.

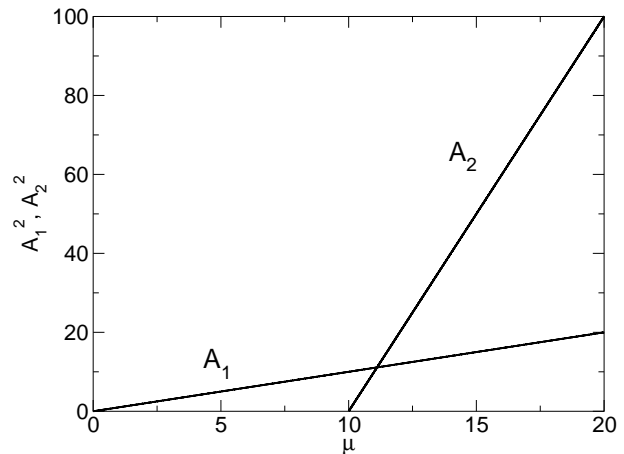


FIG. 3. Bifurcation of pure solutal ( $A_1$ ) and pure thermal ( $A_2$ ) rolls of the model eqs. (3). Parameters are  $a = 10$ ,  $\mu_0 = 100$ , and  $b_1 = b_2 = 1$ .

As the only convective solution for small  $\mu$ , the solutal rolls are stable at onset. But the linear stability analysis shows that they lose stability in favor of the stronger thermal rolls at larger  $\mu$ . The stability is transferred via a third kind of rolls, the intermediate or  $A_1 A_2$ -rolls given by

$$\begin{aligned} A_1^2 &= \frac{b_2 \mu_1 - d_1 \mu_2}{b_1 b_2 - d_1 d_2} \\ A_2^2 &= \frac{b_1 \mu_2 - d_2 \mu_1}{b_1 b_2 - d_1 d_2} . \end{aligned} \quad (8)$$

These structures exist if there is an  $\mu$ -interval where both right-hand sides are  $> 0$ , what is always the case. If  $b_1 b_2 - d_1 d_2 > 0$  they bifurcate forward from solutal to thermal rolls.

A bifurcation diagram showing all three kinds of solutions and also their stability properties within the restricted system (5) is shown in Fig. 4. Plotted is only the interesting  $\mu$ -range where stability is transferred. The stable branches already look like a caricature of the roll branch in the full system with different slopes in the Soret and Rayleigh regions. However, there are also important qualitative differences. In the full system, the roll branch consists of one continuous structure, without the two bifurcation points that are found in the model system.

These bifurcation points will disappear when we break the artificial symmetry present in the model system.

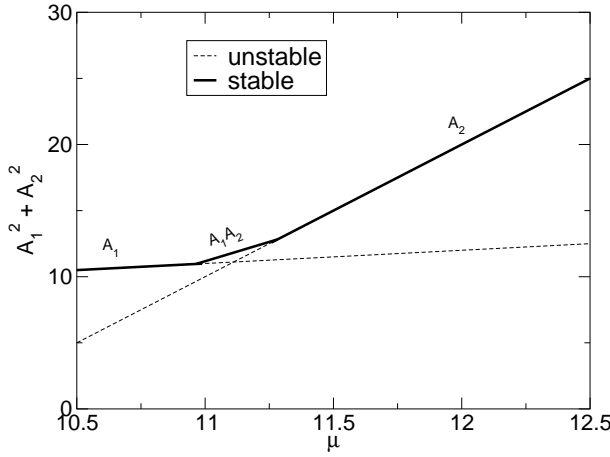


FIG. 4. The three types of stationary rolls solutions of the model eqs. (3): Solutal rolls ( $A_1$ ), thermal rolls ( $A_2$ ) and intermediate rolls ( $A_1A_2$ ) plotted as  $A_1^2 + A_2^2$  versus  $\mu$ . Solid (dashed) lines denote stable (unstable) structures. Parameters are  $d_1 = d_2 = 0.88$  and otherwise as above.

### 3.2 Thermal and solutal squares

A solution has square symmetry when  $A_1 = B_1$  and  $A_2 = B_2$ . Analogous to rolls there are three different types of squares, namely solutal or  $A_1B_1$ -squares

$$A_1^2 = B_1^2 = \frac{\mu_1}{b_1 + c_1}, \quad A_2 = B_2 = 0, \quad (9)$$

thermal or  $A_2B_2$ -squares

$$A_2^2 = B_2^2 = \frac{\mu_2}{b_2 + c_2}, \quad A_1 = B_1 = 0, \quad (10)$$

and intermediate  $A_1B_1A_2B_2$ -squares

$$\begin{aligned} A_1^2 = B_1^2 &= \frac{(b_2 + c_2)\mu_1 - (d_1 + e_1)\mu_2}{\Delta}, \\ A_2^2 = B_2^2 &= \frac{(b_1 + c_1)\mu_2 - (d_2 + e_2)\mu_1}{\Delta}, \end{aligned} \quad (11)$$

where

$$\Delta = (b_1 + c_1)(b_2 + c_2) - (d_1 + e_1)(d_2 + e_2). \quad (12)$$

Under the general requirements stated above the intermediate squares exist and they bifurcate forward from solutal to thermal squares if  $\Delta > 0$ . The bifurcation branches of the different square and roll structures are plotted in Fig. 5.

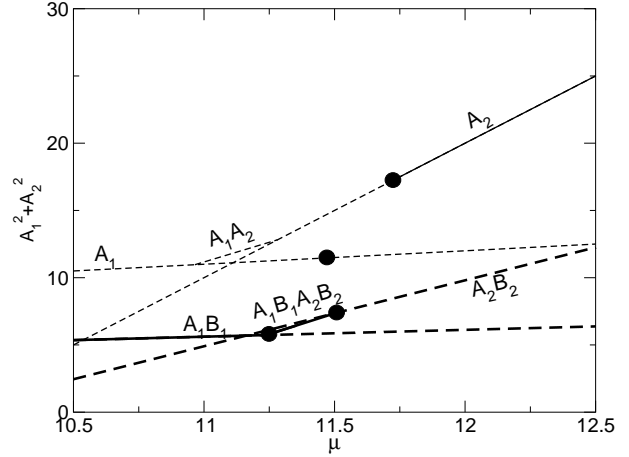


FIG. 5. Square and roll structures of the model eqs. (3). Squares (rolls) are represented by thick (thin) lines. Solid (dashed) lines denote stable (unstable) structures. Bifurcation points of further interest are marked by circles. Parameters are  $c_1 = 0.96$ ,  $c_2 = 1.04$ ,  $e_1 = 0.68$ ,  $e_2 = 1.28$  and otherwise as above.

The stability properties of the different types of squares against each other are analogous to those of the rolls. But these are not all types of possible instabilities. Since our model has four modes four eigenvalues have to be investigated for all structures found so far. We will briefly discuss the respective results.

Some instabilities are connected to the bifurcation points that are known already. For the squares only those instabilities that can break the  $(x \leftrightarrow y)$ -symmetry are still of interest. It turns out that solutal squares are stable against  $(x \leftrightarrow y)$ -antisymmetric  $(\delta A_1, \delta B_1)$ -perturbations everywhere if and only if  $c_1 < b_1$ . This inequality is satisfied in the example case and therefore squares are stable at onset as desired. Similarly, thermal squares are stable against a type of  $(\delta A_2, \delta B_2)$ -perturbations only if  $c_2 < b_2$ . This is not the case and consequently the thermal squares have been marked as unstable in Fig. 5.

These requirements have also consequences for

the stability of rolls: Solutal rolls, although stable against other  $x$ -roll structures for small  $\mu$  are unstable against  $\delta B_1$ -perturbations if and only if  $c_1 > b_1$  as required for solutal squares to be stable. On the other hand, thermal rolls are stable against  $\delta B_2$ -perturbation when  $c_2 < b_2$  and thermal squares are unstable. Therefore, only the thermal rolls are marked as stable in Fig. 5.

There are two other types of instability of rolls that have to be discussed, namely the instability of solutal  $A_1$ -rolls against  $\delta B_2$ -perturbations and vice versa, of thermal  $A_2$ -rolls against  $\delta B_1$ -perturbations. Both instabilities generate new bifurcation points that have been marked by large circles in the figure. Their position depends on the  $d_i$  and  $e_i$ . Due to the fact that  $e_2 > d_2$ , the new bifurcation point on the solutal roll branch lies at higher  $\mu$  than the bifurcation point to the intermediate rolls, where the solutal rolls already lose stability. Since  $e_1 < d_1$ , on the other hand, the new bifurcation point for thermal rolls lies on the otherwise stable part of the thermal roll branch, destabilizing it towards the region of smaller  $\mu$  already before the bifurcation point towards the intermediate rolls.

Placing the new bifurcation points this way no new instabilities are to be expected for the intermediate rolls. They inherit stability against  $\delta B_2$ -perturbations and instability against  $\delta B_1$ -perturbations from the solutal rolls and transfer these properties to the thermal rolls.

It should be pointed out that by choosing the parameters accordingly it is also possible to stabilize the rolls in the whole  $\mu$ -interval against perturbations in  $y$ -direction, which is the scenario that can be found at large  $L$  and small  $\psi$  where the square patterns are always unstable.

Concerning the square structures we have to remark that at the bifurcation point where the intermediate squares branch off from the solutal squares in fact not one but two eigenvalues go through zero for symmetry reasons, namely both  $\delta A_2$ - and  $\delta B_2$ -perturbations. Two types of crossroll branches appear here plus the intermediate squares as nonlinear combination of the two. The same happens at the bifurcation point of the intermediate and thermal squares. Here also two new patterns emerge,

connected to growing  $\delta A_1$ - and  $\delta B_1$ -perturbations. These bifurcation points are also marked by circles as a reminder of the new branches that still have to be discussed.

### 3.3 Crossroll structures

We have already pointed out above that at maximum 16 different stationary structures exist within the model (3). The most simple one is the ground state where all amplitudes vanish. Furthermore we have already discussed the  $A_1$ -,  $A_2$ -, and  $A_1A_2$ -rolls that have their counterpart in  $y$ -direction, i. e., the  $B_1$ -,  $B_2$ -, and  $B_1B_2$ -rolls. Together with the  $A_1B_1$ -,  $A_2B_2$ -, and  $A_1B_1A_2B_2$ -squares these are 10 structures so far. The remaining six are crossroll structures, i. e., three-dimensional patterns lacking the  $(x \leftrightarrow y)$ -symmetry of squares.

The first two of these structures are the  $A_1B_2$ -crossrolls and the  $B_1A_2$ -crossrolls that can be mapped onto each other via the  $(x \leftrightarrow y)$ -symmetry operation. The  $A_1B_2$ -crossrolls connect the  $A_1$ -rolls and the  $B_2$ -rolls at the newfound bifurcation points for the roll structures. Note that  $B$ -roll branches would lie on the  $\mu$ -axis in the plots since only  $A_1^2 + A_2^2$  is plotted. The stability analysis reveals two more bifurcation points on these branches as it has to be since they connect the stable thermal rolls to the twofold unstable solutal rolls.

The next pair are the  $A_1B_1A_2$ - and  $A_1B_1B_2$ -crossrolls that branch off at the connection between solutal and intermediate squares and end up at one of the bifurcation point of the  $B_1A_2$ - and  $A_1B_2$ -crossrolls, respectively.

The  $A_1A_2B_2$ - and  $B_1A_2B_2$ -crossrolls finally emerge at the intermediate squares/thermal squares bifurcation point. These too end up at the  $A_1B_2$ - and  $B_1A_2$ -crossroll branches, at the other two remaining bifurcation points.

That completes the description of the stationary structures. The results are shown in Fig. 6, together with the result of the full stability analysis. The unimportant part of the solutal and thermal roll and square branches have been cut off for better visibility. At small  $\mu$  solutal squares are stable. They lose their stability where two types of

crossrolls ( $A_1B_1A_2$ ,  $A_1B_1B_2$ ) and the intermediate squares branch off. The intermediate squares gain stability whereas the crossrolls are unstable. Taking only stationary structures into account the intermediate squares remain stable until a second bifurcation point, where again two crossroll branches emerge ( $A_1A_2B_2$ ,  $B_1A_2B_2$ ) that are now stable. The thermal squares on the other hand do not gain stability. Next, the stable crossrolls meet a third pair ( $A_1B_2$ ,  $B_1A_2$ ) that finally transfers stability to the thermal rolls. The bifurcation diagram looks qualitatively different for other parameter combinations but the inequalities that have to be fulfilled to produce a diagram as in Fig. 6 can be derived easily.

The picture is still not complete however. Although all stationary instabilities have been identified now, there might be more bifurcation points where time dependent patterns emerge. From the otherwise stable branches only the mixed squares and the  $B_1A_2B_2$ - and  $A_1A_2B_2$ -crossrolls can exhibit oscillatory instabilities. For the given parameters such instabilities do indeed occur. They destabilize the parts of the branches between the circles in Fig. 6. One can easily guess that this is the region where oscillatory crossrolls can be found. But we want to discuss these structures in more detail only in the full model.

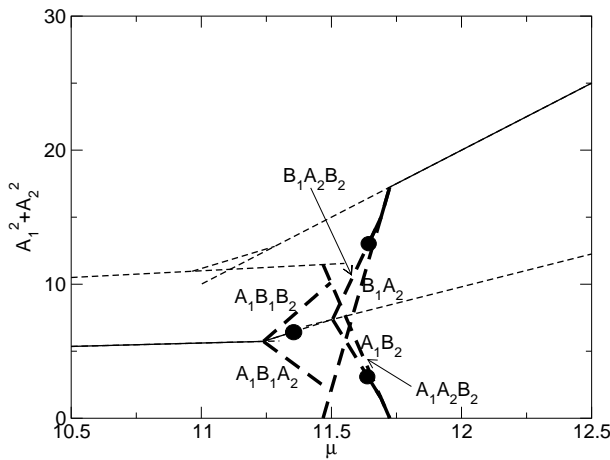


FIG. 6. Stationary crossroll solutions of eqs. (3). Thick (thin) lines represent crossrolls (rolls and squares). Solid (dashed) lines denote stable (unstable) structures. Oscillatory instabilities occur at the circles.

## 4 The full model

The bifurcation diagram we found does already show some of the properties of the scenario we want to explain but turned out to have unwanted bifurcation points. We will now show how including terms that break the artificial extra symmetry leads to a much better model. There are four more cubic terms preserving the symmetries  $(A_1, A_2) \leftrightarrow (B_1, B_2)$ ,  $(A_1, A_2) \leftrightarrow (-A_1, -A_2)$ , and  $(B_1, B_2) \leftrightarrow (-B_1, -B_2)$ . When "..." denotes the old right hand sides of (3) we enlarge the model as follows

$$\begin{aligned} d_t A_1 &= \dots \\ &\quad -A_2(\beta_1 A_1^2 + \gamma_1 B_1^2 + \delta_1 A_2^2 + \epsilon_1 B_2^2) , \\ d_t A_2 &= \dots \\ &\quad -A_1(\beta_2 A_2^2 + \gamma_2 B_2^2 + \delta_2 A_1^2 + \epsilon_2 B_1^2) \quad (13) \\ d_t B_1 &= \dots \\ &\quad -B_2(\beta_1 B_1^2 + \gamma_1 A_1^2 + \delta_1 B_2^2 + \epsilon_1 A_2^2) , \\ d_t B_2 &= \dots \\ &\quad -B_1(\beta_2 B_2^2 + \gamma_2 A_2^2 + \delta_2 B_1^2 + \epsilon_2 A_1^2) . \end{aligned}$$

The new equations do not allow a sign reversal of individual amplitudes anymore. However, the presence of the  $\beta_i$ ,  $\gamma_i$ , and  $\epsilon_i$  alone still allows pure solutal or thermal stationary roll solutions. This leads again to unwanted bifurcation points. On the other hand, when  $\delta_i \neq 0$  such solutions become impossible. We will therefore discuss only these two and set the other six to zero. Thus the model we discuss here is

$$\begin{aligned} d_t A_1 &= \mu_1 A_1 - \delta_1 A_2^3 \\ &\quad -A_1(b_1 A_1^2 + c_1 B_1^2 + d_1 A_2^2 + e_1 B_2^2) , \\ d_t A_2 &= \mu_2 A_2 - \delta_2 A_1^3 \\ &\quad -A_2(b_2 A_2^2 + c_2 B_2^2 + d_2 A_1^2 + e_2 B_1^2) \quad (14) \\ d_t B_1 &= \mu_1 B_1 - \delta_1 B_2^3 \\ &\quad -B_1(b_1 B_1^2 + c_1 A_1^2 + d_1 B_2^2 + e_1 A_2^2) , \\ d_t B_2 &= \mu_2 B_2 - \delta_2 B_1^3 \\ &\quad -B_2(b_2 B_2^2 + c_2 A_2^2 + d_2 B_1^2 + e_2 A_1^2) . \end{aligned}$$

It is instructive to first take a look at the impact that the two new symmetry-breaking terms



have on the eigenvalues of the important branches as they emerge from the linear stability analysis. Fig. 7 shows the real parts of the three most impor-

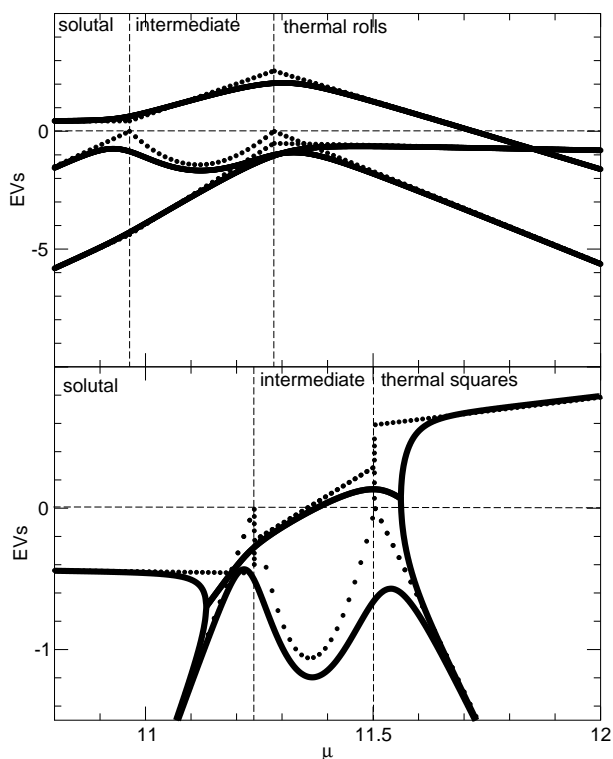


FIG. 7. Eigenvalues (EVs) along the important parts of the different roll and square branches for  $\delta_1 = \delta_2 = 0.01$ . Dots denote the simplified system with  $\delta_i = 0$ .

tant eigenvalues for both rolls and squares for small values  $\delta_1 = \delta_2 = 0.01$  and  $\delta_i = 0$  in comparison. Plotted are the intermediate structures in their  $\mu$ -interval of existence and the solutal and thermal structures below and above, respectively. In the upper plot, one can see how one eigenvalue of the solutal and thermal rolls becomes zero in the simplified system at the points where the intermediate rolls emerge. The referring curves would cross the zero axis here if the picture would not switch to the intermediate rolls. For  $\delta_i \neq 0$  these bifurcations become imperfect. The curves become smooth and do not touch the zero axis anymore such that the two bifurcation points vanish. The respective parts of the solutal, intermediate, and thermal roll branches fuse into one single branch. On the other hand, the bifurcation point to the crossrolls at  $\mu \approx 11.7$

where the rolls finally become stable does not go away when  $\delta_i \neq 0$ .

In the lower plot one can observe a similar behavior for the square eigenvalues. In the simplified system the solutal rolls are stable until one eigenvalue crosses the zero axis and the picture switches to the now emerging intermediate squares. This bifurcation and also that between intermediate and thermal squares becomes again imperfect for  $\delta_i \neq 0$ .

For  $\delta_i = 0$ , at the beginning of the intermediate square interval two eigenvalues approach each other on a very small  $\mu$ -interval such that the curves look discontinuous here. When they meet they form a complex pair and only the real part is shown now. This complex pair becomes critical in the middle of the interval and gives rise to the emergence of the oscillatory crossrolls. After the pair separates rapidly again one eigenvalue goes again through zero. The squares remain unstable because the other eigenvalue remains positive.

Since for  $\delta_i \neq 0$  the bifurcation point between solutal and intermediate squares vanishes, the first crossroll pair that emerges from the squares, the  $A_1B_1A_2$ - and  $A_1B_1B_2$ -crossrolls must become disconnected from the square branch. But the oscillatory bifurcation and the other stationary bifurcation remain. For other parameters the scenario is simpler. All eigenvalues stay real and only one crosses the zero axis. When this is the case, only stationary crossrolls appear.

Note that the pair of eigenvalues responsible for the appearance of oscillatory crossrolls and the eigenvalue of the stationary crossrolls are not independent of each other. The latter emerges from the former. This is a feature that can also be observed in the full system of hydrodynamic field equations.

A bifurcation diagram for slightly different parameters and especially larger symmetry-breaking terms  $\delta_i$  is shown in Fig. 8. The stability properties are the same as in Fig. 1. They are not displayed here. The bifurcation diagram shows all the properties already deducted from the eigenvalues. The lower solutal, intermediate, and upper thermal branches have fused to a smooth curve that nevertheless still shows the characteristic upturning at the transition from the Soret to the Rayleigh regime.

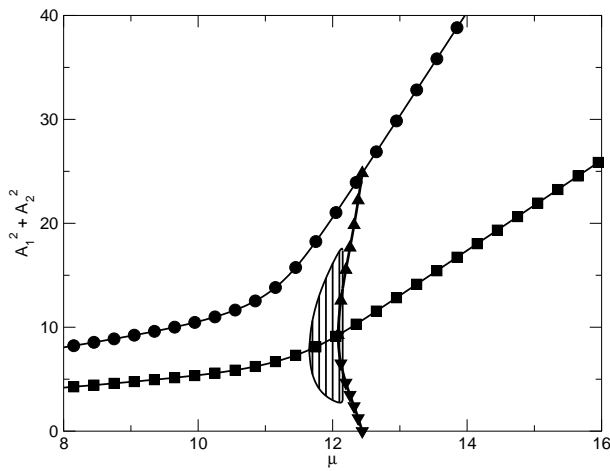


FIG. 8. Bifurcation diagram for  $\delta_i \neq 0$ . Symbols identify rolls, squares, and stationary crossrolls as in Fig. 1. Vertical lines refer to oscillatory crossrolls. The stability properties are not displayed here.

The  $A_1 B_1 A_2$ - and  $A_1 B_1 B_2$ -crossrolls have become disconnected from the square branch. The other stationary crossroll bifurcation does still exist and is preceded by an oscillatory crossroll bifurcation. Qualitatively, the picture is exactly as in Fig. 1.

Before we conclude, we want to take a closer look at the dynamics of the oscillatory crossrolls. Fig. 9 shows oscillations near the beginning (upper plot) and the end (lower plot) of the oscillatory crossrolls branch. Comparing to Fig. 2 one sees the same behavior: An oscillation in counterphase with growing amplitude, decreasing frequency, and growing anharmonicity.

The details of the entrainment process that lead from oscillatory crossrolls to the stationary type shall not be discussed here, but they are different from what we found in the numerical simulations of the full system of field equations [12] although similar transitions have been found in experiments [11].

We found that the details of the dynamic behavior of the model system (14) depends significantly on the chosen parameters. Thus, at present we conclude that our model equations (14) are capable of qualitatively reproducing the bifurcation scenario of Fig. 1 and the dynamics of crossrolls in Fig. 2 as demonstrated in Figs. 8 and 9.

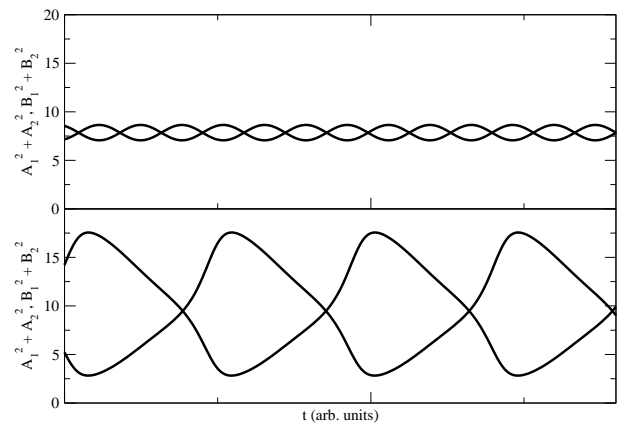


FIG. 9. Oscillatory crossrolls in the model for the parameters of Fig. 8 and  $\mu = 11.66$  (top),  $\mu = 12.14$  (bottom).

## 5 Conclusion

We have investigated the Rayleigh–Bénard convection in binary mixtures with a positive separation ratio. We have shown that the observed bifurcation scenario at small  $L$ , involving square patterns, rolls, stationary and oscillatory crossrolls arises naturally out of a simple system of two coupled amplitude equation systems both consisting of two cubic equations describing the dynamic of rolls in  $x$ - and  $y$ -direction respectively. Attempts to extract such a model from the basic equations are underway.

*Acknowledgement* This work was supported by the Deutsche Forschungsgemeinschaft. We dedicate it to Prof. Dr. Siegfried Großmann on the occasion of his 75th birthday.

## References

- [1] H. Bénard. *Revue générale des Sciences pures et appliquées* **11**, 1261-1271 and 1309-1328 (1900).
- [2] J. W. S. Lord Rayleigh. *Phil. Mag.* **32**, 529 (1916).
- [3] F. H. Busse. *Journal of Mathematics and Physics*, **46** 140 (1967).
- [4] R. M. Clever, F. H. Busse. *J. Fluid Mech.* **65**, 625 (1974).
- [5] F. H. Busse, R. M. Clever. *J. Fluid Mech.* **91**, 319 (1978).

- [6] E. W. Bolton, F. H. Busse, J. Clever. J. Fluid Mech **164**, 469 (1985).
- [7] St. Hollinger, M. Lücke, H. W. Müller. Phys. Rev. E **57**, 4250 (1998).
- [8] J. K. Platten, J. C. Legros. *Convection in Liquids*. (Springer, Berlin, 1984).
- [9] P. Le Gal, A. Pocheau, V. Croquette. Phys. Rev. Lett. **54**, 2501 (1985).
- [10] E. Moses, V. Steinberg. Phys. Rev. Lett. **57**, 2018 (1986); Phys. Rev. A **43**, 707 (1991).
- [11] P. Bigazzi, S. Ciliberto, V. Croquette, J. Phys. (France) **51**, 611 (1990).
- [12] Ch. Jung, B. Huke, M. Lücke. Phys. Rev. Lett. **81**, 3651 (1998).
- [13] B. Huke, M. Lücke, P. Büchel, Ch. Jung. J. Fluid Mech. **408**, 121 (2000).
- [14] T. Clune, E. Knobloch. Phys. Rev. A **44**, 8084 (1992).